

A PROPOSED SUPERFERRIC COMBINED FUNCTION MAGNET

D.E. Lobb and P.A. Reeve

TRIUMF, Physics Department, University of Victoria  
Victoria, B.C., Canada V8W 2Y2

Summary

A design is presented for a rectangular aperture superferric combined function magnet with the dipole and quadrupole field components separately controllable. The coil configuration has been chosen to minimize the total current required and to avoid currents flowing in opposite directions in adjacent conductors. To achieve the necessary fields and gradients, superconducting coils are used and, to maximize the usable field aperture, the coil is cooled using forced cooled supercritical helium. Computer calculations of the magnet properties are presented, together with an example beam transport channel based on these magnets.

Magnet Configuration and Field Properties

Magnets which produce superposed dipole and quadrupole fields have been suggested previously for accelerator magnets<sup>1,2</sup>. Typical properties of such magnets are a circular aperture, a fixed field level, and a fixed relationship of the quadrupole to the dipole field components. For a window frame or H dipole configuration, a quadrupole field component can be introduced by pole shaping; this has the great disadvantage that the aperture available to the particle beam is greater on one side of the magnet than on the opposite side. Magnets intended for beam transport channels often need a rectangular or elliptical aperture, particularly for a large angle of bend of a dispersed beam, and frequently need to be operated with variable field strengths and variable ratios between the dipole and quadrupole components.

Yamamoto<sup>3</sup> has suggested a coil configuration in which the dipole and quadrupole components are produced independently by separate current sheets. This has the disadvantage that in some locations the currents producing the dipole and quadrupole field components are antiparallel. This disadvantage is avoided by the coil configuration shown in fig. 1.

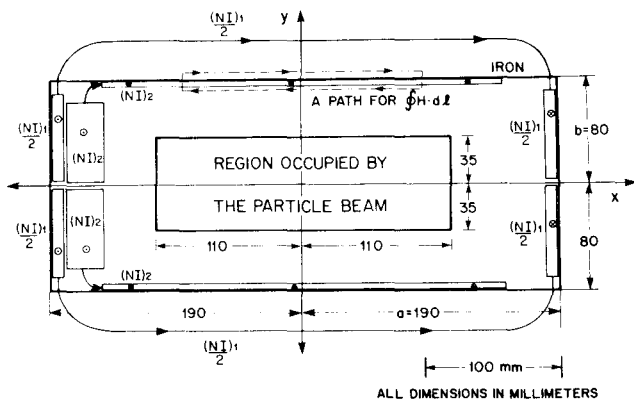


Fig. 1. A schematic diagram of the proposed coil configuration.

For a superposed dipole-quadrupole field the desired field is given by

$$B_x = -gy \tag{1}$$

$$B_y = B_0 - gx \tag{2}$$

where  $B_0 = B_y(0, 0)$  (3)

and  $g = \left. \frac{\partial B_y}{\partial x} \right|_{0,0} = \left. \frac{\partial B_x}{\partial y} \right|_{0,0}$  (4)

It is necessary that  $|ga| > |B_0|$  where  $a$  is the half-width of the horizontal iron surface; this is not a practical restriction. All possible field configurations can be obtained by reversing all current directions and/or rotating the magnet 180° about the  $y$ -axis. For this reason we consider magnets whose pole surface area is bounded by a rectangle.

In the lowest level of approximation we neglect the coil thickness, iron saturation, and the fact that the coil width may be less than the available width of the iron surface. If we evaluate  $\int_C \vec{H} \cdot d\vec{l} = [\text{Total current enclosed by } C]$  for four suitable contours (one such contour is indicated in fig. 1) we obtain

$$(NI)_1 = \frac{2b}{\mu_0} [B_0 - ay] \tag{5}$$

$$(NI)_2 = \frac{2ab}{\mu_0} y \tag{6}$$

$$(NI)_1 + 2(NI)_2 = \frac{2b}{\mu_0} [B_0 + ay] \tag{7}$$

so  $(NI)_1 + (NI)_2 = \frac{2b}{\mu_0} B_0$  (8)

where  $(NI)$  represents the total ampere turns in a coil. Note that  $(NI)_1$  has a smaller value than it does for a pure dipole ( $g=0$ ) field.

In fig. 2 we present the iron and vacuum chambers for such a magnet. This design, referred to as M1, features an asymmetric iron design to keep the average field in the two side yokes approximately the same. It is desired to have  $B_0 \sim 2.3$  T with  $g \sim 9.3$  T/m over  $-11 < x < 11$  cm and  $-3.5 < y < 3.5$  cm (refer to the beam line of fig. 4). Another design, M2, for this beam line features a symmetrical iron design,  $B_0 \sim 2.5$  T, a weak gradient ( $g \sim 1.5$  T/m) over a large volume:  $-10 < x < 10$  cm,  $-7.5 < y < 7.5$  cm. The program GFUN<sup>4</sup> was used to calculate the two dimensional field distribution produced for various current settings in the two configurations. The median plane ( $y = 0$ ) is set to be a plane of geometrical symmetry resulting in  $B_y(x,y) = B_y(x,-y)$ ,  $B_x(x,y) = -B_x(x,-y)$ .

The field values on a semicircle, centered at the origin, were analyzed into Fourier components

$$B_\theta(r, \theta) = a_n r^{n-1} \cos(n\theta) \tag{9}$$

where  $r = \sqrt{x^2 + y^2}$ ,  $\theta = \tan^{-1}(y/x)$ . (10)

The dipole and quadrupole field components for both magnets are presented in table 1; the current values considered are  $\pm 10\%$  about the central value. It can be seen that the desired separated function behavior has been achieved: the dipole component  $B_0$  is quite insensitive to the value of  $(NI)_2$  and the quadrupole component  $g$  is quite insensitive to the value of  $[(NI)_1 + (NI)_2]$ . Over the narrow range of current settings considered,  $B_0$  and  $g$  are, to a good approximation, linear functions of  $[(NI)_1 + (NI)_2]$  and  $(NI)_2$  respectively.

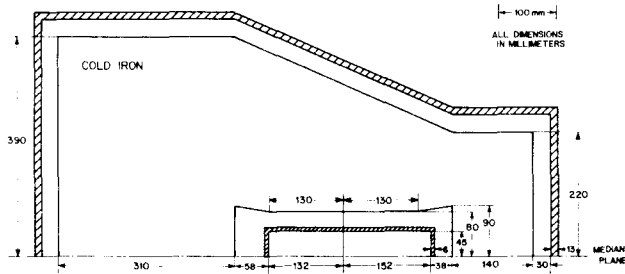


Fig. 2. The iron and vacuum chambers for the magnet M1.

Table 1. GFUN calculated field dipole and quadrupole components for the magnet configurations M1 and M2 for various current settings.

M1 Magnet

$(NI)_1 + (NI)_2$ (kA turns)		$(NI)_2$ (kA turns)		
		155.7	173.0	190.3
270.0	$B_0$ (T)	-2.106	-2.105	-2.105
	$g$ ( $T m^{-1}$ )	8.603	9.555	10.505
300.0	$B_0$ (T)	-2.339	-2.338	-2.337
	$g$ ( $T m^{-1}$ )	8.599	9.549	10.497
330.0	$B_0$ (T)	-2.571	-2.570	-2.570
	$g$ ( $T m^{-1}$ )	8.591	9.540	10.488

M2 Magnet

$(NI)_1 + (NI)_2$ (kA turns)		$(NI)_2$ (kA turns)		
		42.3	47.0	51.7
432.0	$B_0$ (T)	-2.267	-2.267	-2.267
	$g$ ( $T m^{-1}$ )	1.387	1.541	1.689
480.0	$B_0$ (T)	-2.517	-2.517	-2.517
	$g$ ( $T m^{-1}$ )	1.385	1.537	1.698
528.0	$B_0$ (T)	-2.767	-2.767	-2.767
	$g$ ( $T m^{-1}$ )	1.382	1.536	1.690

The harmonic analysis results are insensitive to the radius used in the calculation and agree to a high order of accuracy with the central field and the central gradient [ $g \equiv B_x(0, \Delta y)/(\Delta y)$ ] calculated directly by GFUN.

The simple formulae eqs. (5) to (8) give only rough indications as to the actual field values: coil thickness, iron saturation, and coil width are significant.

To date, an optimum field configuration has not been achieved. For M1 it has been found that variations of the pole profile can reduce the sextupole and octupole field components to tolerable levels;  $a_5$  can be reduced by leaving current-free gaps in the coil;  $a_6$  has been found to be insensitive to these changes.

It is of interest to compare the GFUN-calculated  $|\vec{B}|$  to the value of  $|\vec{B}|_{FIT}$  calculated using eqs. (1) and (2) with the parameters  $B_0$  and  $g$  being obtained from the GFUN-calculated central field values or the GFUN-calculated dipole and quadrupole harmonics. Along the line  $x = -11$  cm,  $-3.0 < y < 3.0$  cm, and over the region  $-6 < x < 6$  cm,  $-3.5 < y < 3.5$  cm, these values differ in magnitude by  $< 1\%$ . For  $x > 6$  cm, the GFUN-calculated field value are a few percent greater than the predictions of the fit: this shows the effect of the lesser saturation in the iron adjacent to the lower field values.

Superconducting Magnet Design

Because peak fields are as high as 3 T, the coil must be superconducting. The magnet is small, so to get the largest ratio of internal gap size to external dimensions, it was decided to use forced cooling with supercritical helium and a cold yoke. The magnet has a warm gap. The advantage of using supercritical cooling is that the cryostat is much less bulky than for pool boiling; the disadvantage is that a complex refrigerator is required. The disadvantages of using a cold yoke instead of a warm yoke are that the heat losses are greater and cool-down time is longer. However, for our purpose, the overwhelming advantage is that the usable gap volume is much larger.

A cross section of the coil and cryostat is shown in fig. 3 and a summary of the parameters is given in table 2. The coil is not cryostable; therefore if a quench occurs, the energy in the coil has to be dumped in an external resistor in less than 2 secs. The NbTi has a copper stabiliser (Residual Resistance Ratio  $> 130$ ) of sufficient mass to limit temperature rise in the conductor to  $< 100$  K if a quench occurs. Calculations with the programs QUSIMT and QUSIMPS<sup>5</sup> indicate that if a quench occurs the maximum temperature will be 12 K and the maximum pressure in the helium will rise from the normal 10 bar to 46 bar. The vacuum chamber walls are relatively thin because they only have to withstand a pressure of only one bar instead of ten bar as in a pool boiling design.

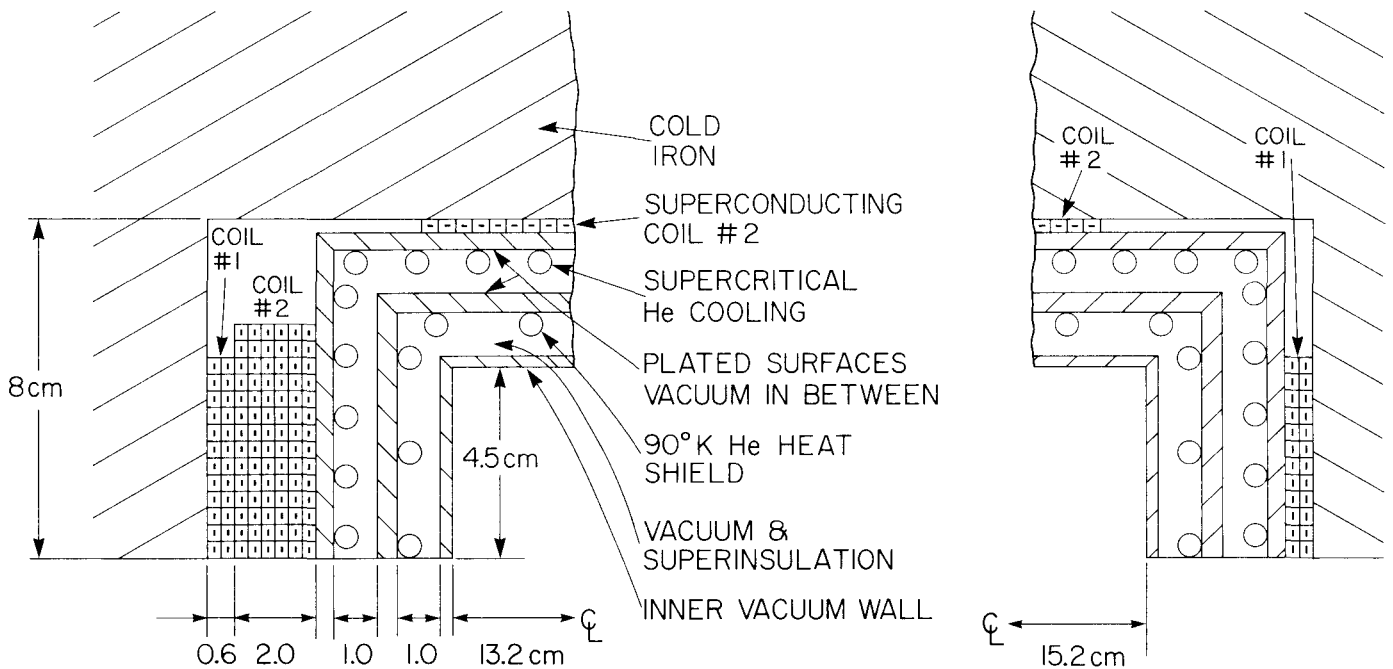


Fig. 3. Details of the coil and cryostat for magnet M1

Simple calculations indicate that the side coils should be self supporting against magnetic stresses. For the top and bottom coils, the stresses are in the direction of their largest dimension, so should not be a problem. The effect of asymmetric forces caused by steel-coil interactions has not been calculated yet.

It is planned that the insulation between the superconducting coil and the heat shield will consist of an evacuated space with no superinsulation, but with chromium or gold plated surfaces on the vacuum box walls. Measurements by Leung et al.<sup>6</sup> show that this method of insulation gives lower heat losses than the conventional method using superinsulation. We are currently repeating and extending these measurements. The heat shield will be cooled with 90 K helium gas. The insulation around the heat shield will be conventional. It is estimated that the radiation losses should be less than 5 W, with negligible convection losses. The major heat loss will be in the current leads, about 9 W. This could be reduced by using a lower current, but the coil would be larger and therefore the usable gap space would be smaller. A liquid helium flow rate of 2.3 g/s through a 5 mm diameter tube of approximately 50 m will cause a small pressure drop of about one tenth of a bar, with frictional heating of less than 0.2 W.

Table 2. Summary of superconducting coil parameters

PARAMETER	VALUE
Maximum field (in coil)	3.5 T
Current	2500 A
Superconductor current density	2100 A/mm <sup>2</sup>
Stabiliser current density	245 A/mm <sup>2</sup>
Ratio copper to NbTi	8.5 : 1
Maximum magnetic stress (in coil)	$1.7 \times 10^8$ N/m <sup>2</sup>
Quench time	2 s
Estimated heat losses	< 15 W

A Proposed Beam Transport Channel using These Magnets

The decay length of 0.55 GeV/c kaons is 4.13 m; only 38% survive a 4 m drift. In fig. 4 we present a channel in which the combined function magnets allow a channel length much shorter than would be the case for a separated function design. This channel represents a new version of part of a channel presented previously<sup>7</sup>.

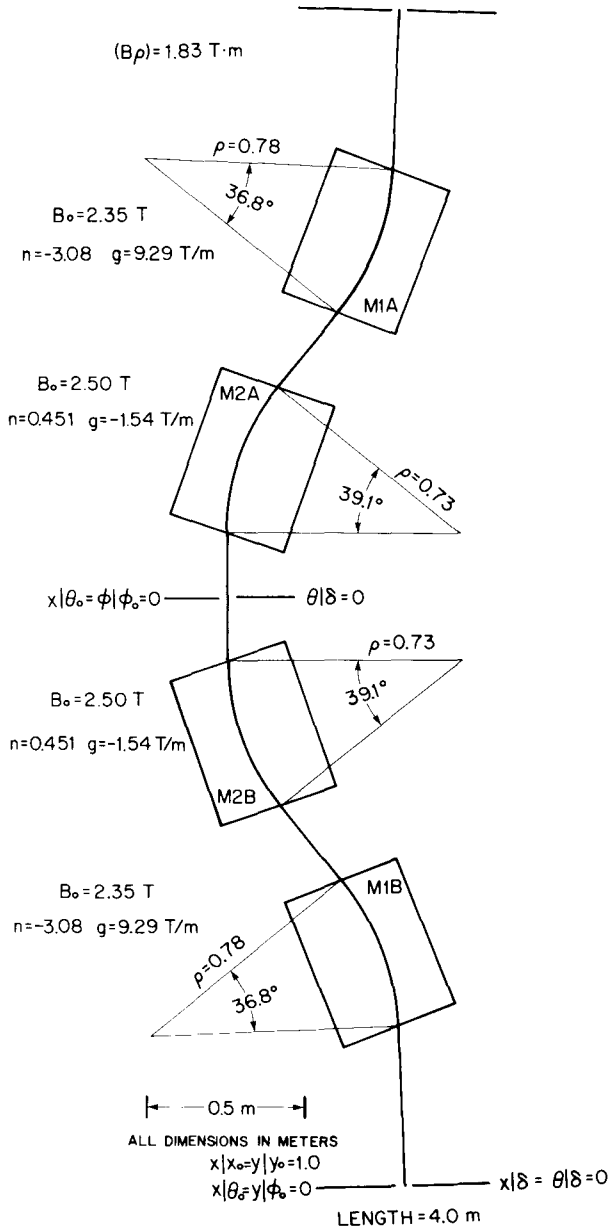


Fig. 4. A proposed 0.55 GeV/c channel utilizing combined function magnets.

Conclusions

Much work remains to be done to improve the field quality and calculations need to be done on the properties of the three-dimensional field produced by short, large aperture magnets. However, the work to date indicates that superferric magnets with separately controllable dipole and quadrupole field components could play a role in channels where space is at a premium: the combined function feature means fewer magnetic elements in the channel and the superconducting coils allow higher magnetic fields and hence shorter elements. The engineering parameters of such magnets are well within the capability of contemporary technology.

REFERENCES

1. J.H. Coupland, Nucl. Instr. and Meth. 78 (1970) 181
2. H. Hahn and R.C. Fernow, IEEE Trans, Nucl. Sci. NS-30 (1983) 3402
3. A. Yamamoto et al., Proceedings of the Kaon Factory Workshop, TRIUMF Report TRI-79-1 (1979)212
4. A.G.A.M. Armstrong, Rutherford Laboratory Report RI-76-029/A (1976)
5. C. Marinucci, Private Communication (1981)
6. E.M.W. Leung et al., in Advances in Cryogenic Engineering, K.D. Timmerhaus and K.D. Snyder, eds., Plenum Press. 25 (1980) 489
7. D.E. Lobb, IEEE Trans, Nucl. Sci. NS-30 (1983) 2827